Journal of Applied Polymer Science

Thermomechanical properties and water uptake capacity of soy protein-based bioplastics processed by injection molding

Lucía Fernández-Espada, Carlos Bengoechea, Felipe Cordobés, Antonio Guerrero
Departamento De Ingeniería Química, Universidad De Sevilla, Facultad De Química. Profesor García González 1, Sevilla 41012, Spain
Correspondence to: C. Bengoechea (E-mail: cbengoechea@us.es)

ABSTRACT: The optimization of the processing conditions in the production of soy protein bioplastics by injection molding has been essential in order to develop materials with a great capacity to absorb water while displaying good mechanical properties. Using a 50/50 (wt/wt) soy protein/glycerol mixture, and 40 °C, 500 bar, and 70 °C as reference values for cylinder temperature, injection pressure, and mold temperature, respectively, the effect of those processing parameters over thermomechanical and hydrophilic properties was studied. Processing parameters did not show a great influence over the thermomechanical bending properties within temperatures ranging from −30 to 130 °C, as most samples displayed a similar response, independently of the parameter studied. On the other hand, when studying tensile and hydrophilic properties, the main effect corresponded to the cylinder and mold temperature values, as pressure did not exert a clear influence when increased from 300 to 900 bar. Samples with a lower water uptake were obtained when processed at higher temperature, as a result of crosslinking promotion. Moreover, a greater extensibility was observed when bioplastics are processed at high mold temperatures. © 2016 Wiley Periodicals, Inc. J. Appl. Polym. Sci. **2016**, *133*, 43524.

KEYWORDS: crosslinking; hydrophilic polymers; mechanical properties; molding; proteins

Received 9 October 2015; accepted 8 February 2016
DOI: 10.1002/app.43524

INTRODUCTION

Traditionally, most plastic products to be used in a great variety of applications (e.g., packaging, construction, electronic devices, houseware, etc.) have been made from synthetic materials derived from petroleum, such as polyethylene, polypropylene, polystyrene, and so forth. As most of them cannot be degraded easily, eventually resulting in serious environmental and ecological consequences, they are being gradually replaced by bioplastics. Interest in protein-based bioplastics has increased enormously due to their excellent potentials derived from a series of factors such as low cost, high profitability and availability, and excellent biodegradability.[1]

Protein from soybean is one of the most used biopolymer raw materials for bioplastics production, as it is a renewable source with an affordable price. Soy contains approximately 40% of protein, 20% of oil, 35% of carbohydrates, and 5% of ashes (referred to dry matter).[2,3] Several soy products with different protein content are generally available: soy protein isolate (SPI, 90%), soy protein concentrate (SPC, 72%), soy flour (SF, 56%), and soy meal[4] (SM, 48%). Soy protein possesses a complex structure, where glycine (7S) and β-conglycinin (11S) represent the major fractions, being composed of 20 aminoacids, with different SH, [&bond]OH and [&bond]NH side groups that facilitate cross-linking reactions with other polymers.[5–8] Soy proteins are typically hard to process unless a certain amount of plasticizers, denaturing agents, or a combination of both of them is present in the formulation of the bioplastic material. Plasticizers are low molecular weight agents that show the ability to increase the protein chains mobility, reducing the number of intra and intermolecular interactions. Water and polyalcohols are widely used as plasticizers for soy protein, of which glycerol is the most often used from this group.[9–13]

Injection molding, along with extrusion ranks as one of the prime processes used in the plastics industry. This polymer processing technique provides efficient, simple, and fast preparation and is used to produce large numbers of identical items from high precision engineering components to disposable consumer goods, being very adequate to achieve a high-volume production. Nowadays, a wide variety of products are manufactured using injection molding, which vary greatly in their size, complexity, and application. Injection molding is a batch process that consists of three different stages. Typically, the first one is a plasticization stage to obtain a polymer melt. The second stage is mold filling which comprises injection and compression (at controlled injection rate and pressure) and holding (at controlled pressure and residence time in the mold). The last stage

involves cooling of the sample. The injection process performed in a lab-scale injection machine is basically the same, but the plasticization is performed in a small cylindrical chamber, fitted with a piston, instead of a screw and barrel system. Most of applications for injection-molded materials have been developed for thermoplastic polymers. However, processing may be very different for protein-based materials, for which no many data are available.[14,15] Thus, excessive temperature should be avoided in the cylinder to prevent crosslinking formation, whereas high temperature would be imposed at the mold in order to favor reticulation of the protein network.[14,15]

It has been reported how the most influential processing parameters are the injection temperature (also referred as cylinder temperature), the molding temperature and pressure.[15–18] However, the selection of those processing parameters to achieve optimal mechanical properties of the bioplastics is far from trivial. In any case, applications to obtain soy protein-based plastics are still limited because of its low strength and high moisture adsorption.[19,20]

This work focuses on the impact of those processing parameters required for the manufacture of soy protein-based bioplastics through injection molding: mold temperature, injection temperature and injection pressure. The adequate selection of the optimal processing parameters is a key factor to obtain bioplastics showing properties that are suitable for their end-use application. In this study, thermomechanical bending and tensile properties, as well as water uptake capacity of the manufactured bioplastics have been studied.

EXPERIMENTAL

Materials

Soy protein isolate (SPI, min. 90% protein content) was supplied by Protein Technologies International (SUPRO 500E, Leper, Belgium). The protein content was determined in quadruplicate as % $N \times 6.25$ using a LECO CHNS-932 nitrogen microanalyzer (Leco Corporation, St. Joseph, MI) being 91 wt %. Glycerol (GL) from Panreac Química, S.A. (Spain) was used as plasticizer in the bioplastic formulation.

Sample Preparation

The SPI/GL blends (50/50) were properly mixed using a Brabender Plastograph, PL 3s model (Germany), which could be used in batch processing operations and which provided the agitation necessary to obtain a well integrated mixture of the components. The equipment was fitted with a roller-type head with two-delta shape, counter-rotating blades turning with different angular velocities. A detailed description of this equipment and its operational conditions may be found in the bibliography.[21,22] The angular velocity of the slower blade was 50 rpm, and the blending process took 10 min in all cases. The blend was produced at room temperature, under adiabatic conditions, following the same protocol as in previous papers.[23] Samples were frozen in sealed plastic bags prior to its injection.[24] A suitable proportion of 50% of glycerol as plasticizer agent has been selected in order to obtain an adequate viscosity for blends.

Table I. Summary of the Processing Conditions used in Injection Molding for SPI/Gly Bioplastics, 50/50

Cylinder temperature (°C)	40		
	80	40	40
	120		
Injection pressure (bar)		300	
	500	500	500
		900	
Mold temperature (°C)			60
	70	70	70
			80
			90

The materials obtained after the mixing process were subsequently processed by injection molding using a MiniJet Piston Injection Molding System (ThermoHaake, Karlsruhe, Germany) to obtain bioplastic probes. The most suitable processing variables, such as injection temperature and pressure, as well as residence time in the preinjection mixing chamber, were selected after performing temperature ramp and time sweep tests to the dough-like materials. Three types of molds were used to prepare the probes: a 60 × 10 × 1 mm rectangular shape mold for DMTA experiments; a dump-bell type probe (thickness: 2 mm) defined by ISO 527-2:1993 for Tensile Properties of Plastics; and a circular shape mold (25 × 1.5 mm^2) for water uptake measurements.

The processing parameters selected in order to study the influence over the mechanical and physical properties of the resulting SPI/GL bioplastics were: cylinder temperature, injection pressure, and mold temperature. Table I shows every processing condition studied in the present manuscript.

Density of bioplastic samples was estimated after weighing samples in an Ultra Mark digital laboratory balance (BEL Engineering) and measuring its dimensions using a micrometer IP65 (Mitutoyo).

Dynamic Mechanical Analysis

Dynamic mechanical analysis (DMA) experiments were performed with a RSA3 rheometer (TA Instruments, New Castle, DE) using a cylindrical compression geometry (compression mode) for the SPI/GL mixture used to feed the injection molding system, and then in a dual cantilever bending mode (tension mode) for the SPI/GL bioplastics obtained from injection molding through different processing conditions (cylinder temperature, injection pressure, and mold temperature). All samples studied contain the same amount of plasticizer (50%).

Strain sweep tests were performed to determine the linear viscoelastic region (LVR) (between 0.01 and 0.3%). Dynamic temperature sweeps were performed at a constant frequency of 1 Hz and strains within the linear viscoelasticity region. The heating rate was set at 3 °C/min, within a temperature interval from −30 to 130 °C. All the bioplastic samples were coated with Dow Corning high vacuum grease to avoid water loss. At least two replicates of each measurement were performed on samples

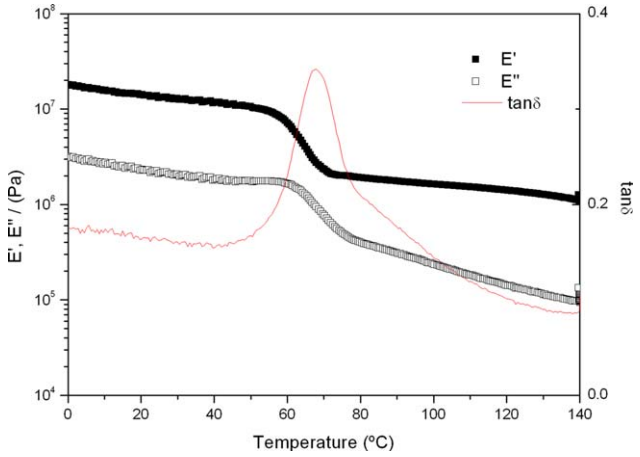

Figure 1. Evolution of E' and E'' and tanδ with temperature for a SPI/Gly 50/50 mixture processed in a Brabender Plastograph, PL 3s model for 10 min at 50 rpm. [Color figure can be viewed in the online issue, which is available at wileyonlinelibrary.com.]

24 h after of the manufacture and are reported as means and standard deviations. Prior to their characterization, samples were stored at room temperature in a sealed flask.

Tensile Tests

Tensile tests were performed with a 10 kN Electromechanical Testing System (MTS, Eden Prairie, MN), according to ISO 527-2:1993 (Tensile Properties of Plastics) with an extension rate of 1 mm/min, at room temperature. An extensometer was used in order to accurately register the sample elongation. At least five tests were carried out on samples 24 h after of the bioplastic manufacture and are reported as means and standard deviations.

Water Uptake and Soluble Matter Loss

Water absorption tests, according to ASTM D570 (2005), were carried out on circular probes immersed into distilled water for 24 h. The water absorption percentage was calculated as:

$$\text{Water absorption (wt\%)} = \frac{\text{wet wt} - \text{reconditioned wt}}{\text{conditioned wt}} \times 100 \quad (1)$$

where conditioned wt, is the initial weight of the probe; wet wt, refers to the weight of the probe just after 24 h of water immersion; reconditioned wt, is the final weight of the wet sample after 24 h of drying in an oven at 50 °C.

Moreover, soluble matter loss was estimated as:

$$\text{Soluble matter loss (wt\%)} = \frac{\text{conditioned wt} - \text{reconditioned wt}}{\text{conditioned wt}} \times 100 \quad (2)$$

At least two replicates of each measurement were performed on samples 24 h after of the bioplastic manufacture and are reported as means and standard deviations.

Scanning Electron Microscopy

Microstructure of selected bioplastic samples was determined in collaboration with the Microscopy Service (CITIUS, Universidad de Sevilla, Sevilla, Spain) as described by Orawan *et al.*[25] Samples with a thickness of 1.5 mm were mounted on a bronze stub, and sputter-coated with gold. The specimens were observed with a Philips XL-30 Scanning electron microscope (SEM; Eindhoven, the Netherlands) at an acceleration voltage of 10 kV.

RESULTS AND DISCUSSION

Dynamic Mechanical Analysis

Figure 1 shows the evolution of the elastic and viscous moduli obtained for the SPI/GL mixture when it was heated from 0 to 140 °C, always prevailing the elastic component (E') over the viscous one (E''). It is clear that a softening of the mixture takes place as temperature rises, leading to a maximum of the loss tangent, tanδ, around 68 °C, which presumably corresponds to a glass transition of the sample. It may seem plausible, that the optimum temperature for the injection processing of this

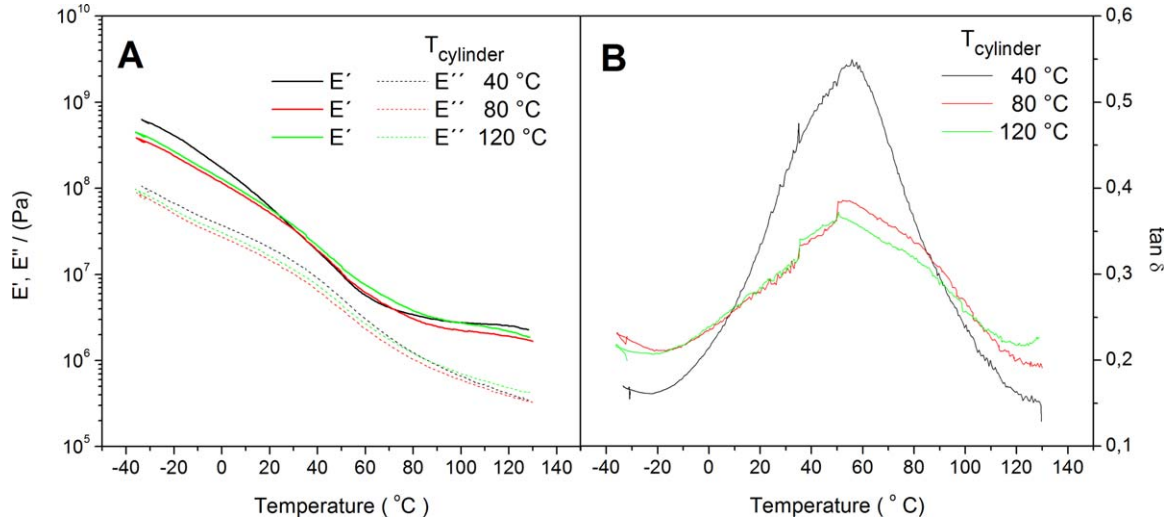

Figure 2. Evolution of E' and E'' (A) and tanδ (B) with temperature for SPI/Gly 50/50 probes processed through injection molding at different cylinder temperatures (40, 80, and 120 °C), with an injection pressure of 500 bars, and a mold temperature equal to 70 °C. [Color figure can be viewed in the online issue, which is available at wileyonlinelibrary.com.]

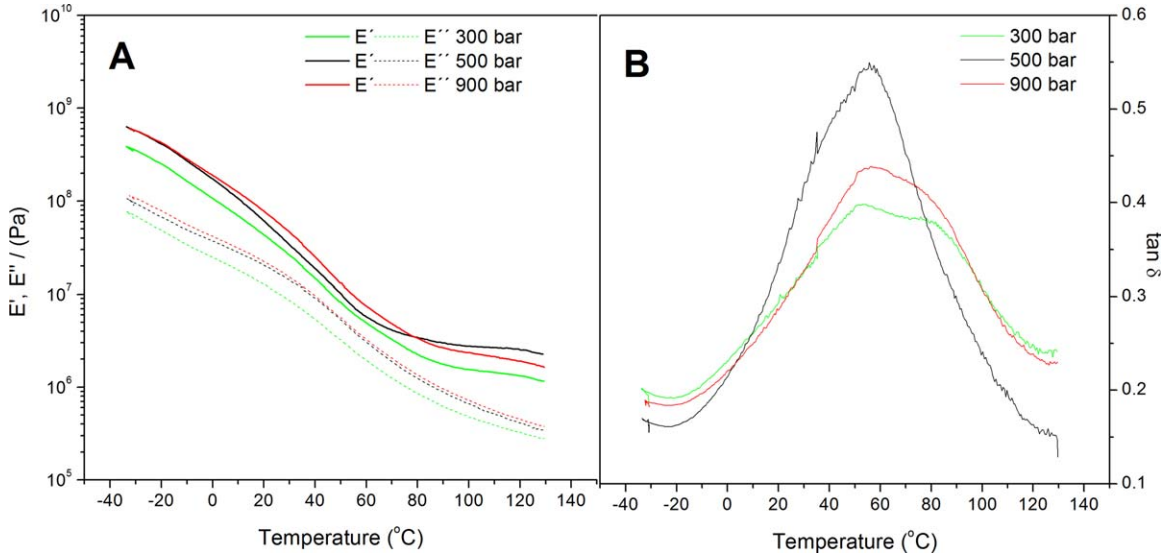

Figure 3. Evolution of E' and E'' (A) and tanδ (B) with temperature for SPI/Gly 50/50 probes processed through injection molding at different injection pressures (300, 500, and 900 bars), with an cylinder temperature of 40 °C, and a mold temperature equal to 70 °C. [Color figure can be viewed in the online issue, which is available at wileyonlinelibrary.com.]

mixture would be that corresponding to the minimum value of the elastic component, as the flow of the protein-plasticizer mixture from the injection chamber into the mold would be favored then. On the other hand, it should be taken into account that exposition of blends to high temperature may promote heat-induced protein crosslinking. In fact, a decrease in the loss tangent may be appreciated in Figure 1 at high temperature, even though no minimum in E' is reached, which is consistent with the results shown previously.[14] This may be regarded as a consequence of a higher thermoplastic character shown by SPI, especially when compared to other proteins, such as gluten[26] or egg albumen.[14] In any case, it also seems clear that there is a wide temperature window available for the processing of this protein, which provides a high flexibility in the selection of the injection temperature.

Bioplastics obtained through injection molding from the mixture were also characterized through DMA tests, though now in dual cantilever mode. Thus, the influence of different processing parameters (cylinder temperature, injection pressure and mold temperature) over their viscoelastic properties was studied. Qualitatively, all the probes show analogous response to temperature independently of the processing conditions [Figures 2(A), 3(A), and 4(A)], always being the elastic modulus (E') higher than the loss modulus (E''), resulting in tanδ values always lower than 1, for the whole temperature range studied (−30 to 130 °C). Both moduli decrease their values as temperature

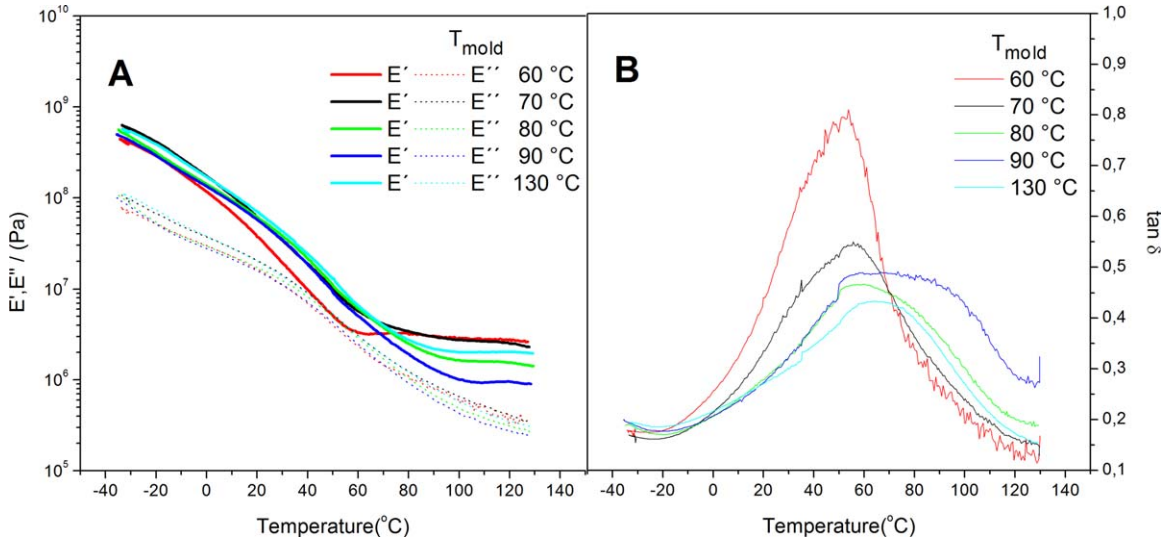

Figure 4. Evolution of E' and E'' (A) and tanδ (B) with temperature for SPI/Gly 50/50 probes processed through injection molding at different mold temperatures (60, 70, 80, 90 °C), and with an injection pressure of 500 bars, and a cylinder temperature of 70 °C. [Color figure can be viewed in the online issue, which is available at wileyonlinelibrary.com.]

Table II. $T_{\alpha 2}$ and Tan δ_2 Values for the Different Processing Conditions used in Injection Molding for SPI/Gly Bioplastics, 50/50

		$T_{\alpha 2}$ (°C)	tanδ ($T_{\alpha 2}$)
Cylinder temperature (°C)	40	51 ± 1	0.38 ± 0.01
	80	55 ± 3	0.56 ± 0.07
	120	53 ± 4	0.38 ± 0.02
Injection pressure (bar)	300	53.0 ± 0.6	0.42 ± 0.03
	500	55 ± 3	0.56 ± 0.07
	900	56.1 ± 0.4	0.42 ± 0.01
Mold temperature (°C)	60	54.1 ± 0.2	0.83 ± 0.03
	70	55 ± 3	0.56 ± 0.07
	80	59 ± 2	0.47 ± 0.01
	90	63 ± 3	0.56 ± 0.01
	130	65 ± 4	0.43 ± 0.06

increases, showing a tendency to reach a plateau value. Even though the system studied is a complex mixture of protein molecules and glycerol, this profile is similar to the typical behavior shown by polymers when they are heated, specifically, the glass transition region and rubbery plateau, respectively. All the probes studied also display similar loss tangent profiles [Figures 2(B), 3(B), and 4(B)] showing one single peak in the temperature range tested. Other authors reporting about this peak also indicated occurrence of a previous peak at temperatures lower than −50 °C.[1,27] According to these authors, glycerol-plasticized soy protein plastics could be visualized as blends of plasticizer-rich and protein-rich domains that lead to occurrence of two concomitant α-relaxation events $T_{\alpha 1}$ and $T_{\alpha 2}$, respectively. Therefore, the maximum value on tanδ curves shown in Figures 2(B), 3(B), and 4(B) can be attributed to the glass transitions of protein-rich domains (T_{g2}) for which a good compatibility between protein and plasticizer seems to take place as may be deduced from the unimodal tanδ profile. More specifically, the values obtained for $T_{\alpha 2}$ and tanδ ($T_{\alpha 2}$) are reported to be in the range of 50–75 °C and 0.3–0.5, respectively, for similar SPI/GL ratios.[1,14,27,28,30] The values of $T_{\alpha 2}$ and tanδ peak obtained for the SPI/GL specimens are included in Table II. As may be observed, most of these values fit to the reported ranges for $T_{\alpha 2}$ and tanδ ($T_{\alpha 2}$) as is also the case for the SPI/GL blend.

Figure 2 shows the results obtained for SPI/GL bioplastics processed at different preinjection cylinder temperatures (40, 80, and 120 °C), keeping both the injection pressure and the mold temperature constant (500 bars and 70 °C, respectively). When studying the effect of cylinder temperature, even if no great differences were found [Figure 2(A)], it is noticed how the greatest values for the elastic modulus at low temperatures are obtained at the lowest cylinder temperature (40 °C). Moreover, at that cylinder temperature, the E' drop onto the plateau region is steeper than at 80 or 120 °C, reaching the plateau region at lower temperatures. This may be explained by the thermal behavior previously observed for the mixture, since it is the only sample processed at an injection temperature lower than the glass transition reported for the mixture (68 °C). Thus, viscoelastic properties of the sample fed onto the mold are expected to be higher at 40 °C than those found at 80 or 120 °C, as those conditions may promote a drop in the viscoelastic properties, once the specimens are molded. As commented previously, all the specimens show values that approximately fit into the range found in the literature, though it is observed how the system injected at the lowest temperature (40 °C) shows a less elastic character (i.e., a higher tanδ peak) than those injected at a higher temperature. On the other hand, $T_{\alpha 2}$ remains constant (around 55 °C), independently of the cylinder temperature.

Figure 3 shows the results obtained for SPI/GL bioplastics processed at different injection pressures (300, 500, 900 bars), keeping both the injection temperature and the mold temperature constant (40 and 70 °C, respectively). It is noticed how from −30 up to 80 °C there is a tendency onto higher values of E' and E'' as injection pressure increases from 300 to 900 bars [Figure 3(A)]. This evolution is explained on basis of the fact that higher pressures may cause a higher degree of orientation, which would result in an increase in viscoelastic properties. An increase in density, from 1170 ± 5 kg/m^3 to 1260 ± 40 kg/m^3 for 300 and 900 bar, respectively, as a consequence of the effect of pressure during the packing stage has to be also considered. This evolution, that prevails over the whole temperature range studied for the loss modulus, E'', is altered for the elastic modulus, E', of the sample processed at 500 bars, which shows the highest elastic modulus above 80 °C. The decrease that takes

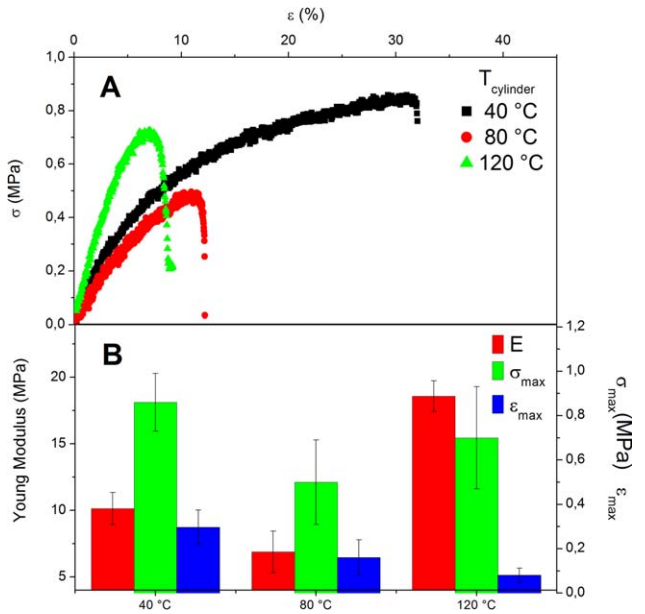

Figure 5. Stress–strain curves obtained from uniaxial strength measurements for SPI/GL bioplastics for three cylinder temperatures (40, 80, and 120 °C) (A). Tensile properties for SPI/Gly 50/50 processed through injection molding at different cylinder temperatures (40, 80, and 120 °C) with an injection pressure of 500 bars, and a mold temperature equal to 70 °C (B). [Color figure can be viewed in the online issue, which is available at wileyonlinelibrary.com.]

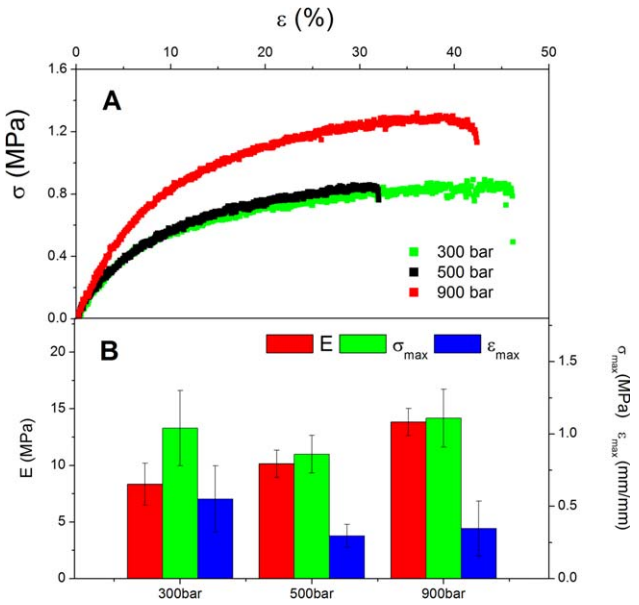

Figure 6. Tensile properties for SPI/Gly 50/50 processed through injection molding with an injection chamber temperature of 40 °C, and a mold temperature equal to 70 °C, and different injection pressure 300, 500, and 900 bars. [Color figure can be viewed in the online issue, which is available at wileyonlinelibrary.com.]

place for E' at higher temperatures when increasing injection pressure to 900 bars is not clear though it may be related to the fact that higher pressure may cause additional denaturing, which could lead to a more amorphous, well-consolidated structure, and thereby lower modulus.[15] No clear tendency is found neither for $T_{\alpha 2}$ or tanδ ($T_{\alpha 2}$) when varying the injection pressure [Figure 3(B)], though the maximum tanδ ($T_{\alpha 2}$) is observed at 500 bars.

Figure 4 shows the results obtained for SPI/GL bioplastics processed at different mold temperatures (60, 70, 80, 90, and 130 °C), keeping both the temperature of preinjection cylinder and the injection pressure constant (40 °C and 500 bars, respectively). When studying the effect of mold temperature, it may be observed how no great influence of mold temperature over E' or E'' was found at low temperatures. At intermediate temperatures (from 20 to 70 °C approximately), no great differences are found for E' or E'' for the different mold temperatures, except for the probe processed at the lowest mold temperature, at which E' shows lower values than the rest. Under such mild conditions the degree of crosslinking obtained over molding seems to be very low. Interestingly, these specimens (molded at 60 °C) reach the plateau region at the lowest temperature, just after the temperature used for the molding conditions was surpassed. In other words, the rubbery plateau is reached at lower temperatures than the rest of systems. In addition, a decrease in E' and E'' with increasing molding temperature is apparent at the high temperature region of DMA plots. As mentioned above, the effect of molding temperature in this region may produce two opposite effects: on one hand an increase in temperature tends to produce a decrease in viscoelastic properties, as observed in the E' profile shown in Figure 1, but on the other, it may also induce crosslinking, previously related to the decrease in tanδ. The first effect seems to be dominant in this high temperature region up to a mold temperature of 90 °C, whereas the second takes place at the highest mold temperature. As a result a minimum may be observed at 90 °C.

It also may be noticed how the onset of the rubbery plateau seems to undergo a shift toward higher temperatures. As a result, the specimens processed at higher molding temperatures show an extension of the E' decreasing region up to higher temperatures. Thus, the plateau region takes place at lower E' values as the molding temperature decreases. This different behavior may be related to the fact that in this case the temperature of the mold is lower than the glass-like transition of the 50/50 blend (Figure 1). In this way, the lower mobility and flexibility of protein chains may limit the development of protein–protein crosslinking. A lower crosslinking degree due to the lower temperature should be also considered. Either way, conditions selected for the injection molding of the SPI/GL blend seem to be suitable in all cases.

As may be seen in Figure 4(B), all the specimens show values that fit into the range found in the literature, excepting the system molded at the lowest temperature (40 °C) that shows a lower elastic character (i.e., a slightly higher tanδ peak). In addition, as mold temperature gets higher, a displacement in the maximum value of the loss tangent onto higher temperatures may be also observed. This behavior may be regarded as a consequence of an increase in the crosslinking degree, but also of a decrease in moisture content both of them induced by the

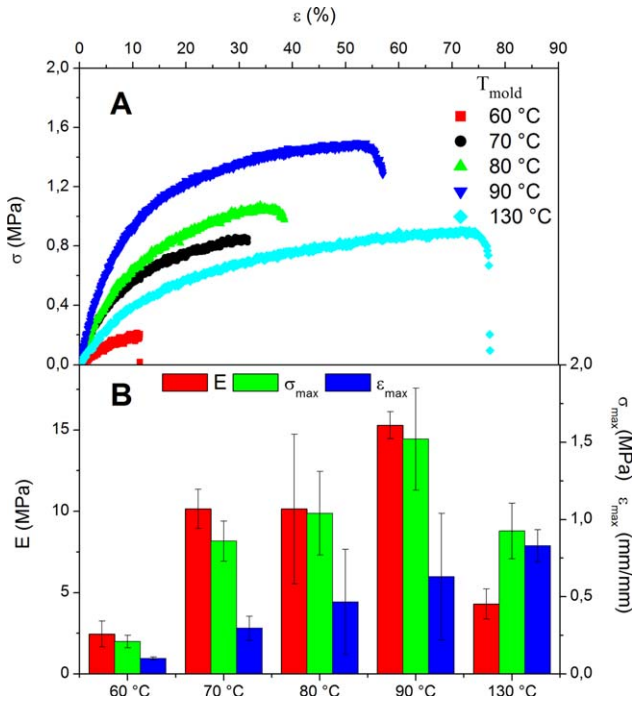

Figure 7. Tensile properties for SPI/Gly 50/50 processed through injection molding with an injection pressure of 500 bars, and a different mold temperature 60, 70, 80, 90 °C, and injection temperature equal to 70 °C. [Color figure can be viewed in the online issue, which is available at wileyonlinelibrary.com.]

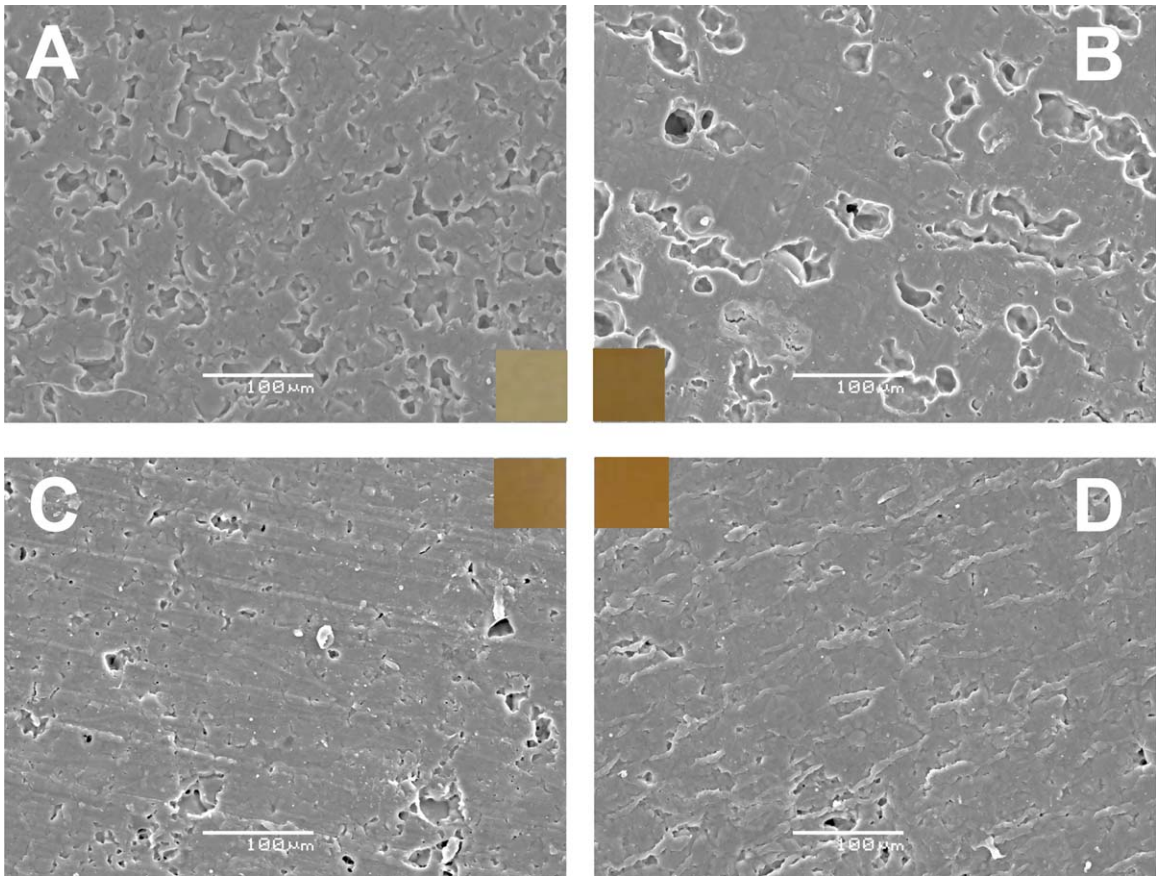

Figure 8. SEM photographs of SPI/Gly 50/50 processed at selected processing conditions (cylinder temperature/injection pressure/mold temperature): (A) 40/500/70; (B) 40/500/90; (C) 40/900/70; (D) 120/500/70. [Color figure can be viewed in the online issue, which is available at wileyonlinelibrary.com.]

increase in molding temperature. A reduction in T_{g2} with increasing moisture content was also reported by Zhang and Zhang, Mungara and Jane[3] for extruded SPI/glycerol sheets, or by Kalichevsky *et al.*[31] for gluten protein. These former authors reported a 5 °C upward shift in the tanδ peak temperature by a loss of 1% in moisture content.

Tensile Tests

Figure 5 shows the results obtained from uniaxial strength measurements for SPI/GL bioplastics. Figure 5(A) displays those results of stress–strain curves obtained for the three cylinder temperatures at which bioplastics were processed. All the curves, including those obtained at different injection pressure and mold temperatures [Figures 6(A) and 7(A)], exhibit an initial linear elastic behavior of constant stress–strain slope yielding different values for the Young's Modulus (E), followed by a plastic deformation stage with a continuous decrease in the stress–strain slope after the elastic limit. All the curves eventually reach a maximum value for the stress (σ_{max}) and the strain (ε_{max}), which is immediately followed by a sudden decrease in stress that corresponds to the rupture of the sample.

Figure 5(B) shows the values of the three parameters (E, σ_{max}, and ε_{max}) from tensile tests performed on SPI/GL bioplastic specimens, as a function of the cylinder temperature. A tendency into a minimum at intermediate temperatures (80 °C) seems clear for E and σ_{max}. This evolution is inverse to that described above for the loss tangent of SPI/GL blends. In other words, the higher the loss tangent shown by the blend, the lower Young modulus (and σ_{max}) obtained for the specimen. Thus, the highest Young modulus is clearly obtained at 120 °C, which may be associated to a higher degree of crosslinking taking place in the cylinder, which may be also related to the fact that after 80 °C, the glass transition region has been fully developed. It may be also noticed that parameter ε_{max} tends to decrease with increasing the temperature of the cylinder.

Figure 6(B) shows the values of E, σ_{max}, and ε_{max} from tensile tests performed on SPI/GL bioplastic specimens, as a function of the injection pressure. An increase in the pressure from 300 to 900 bars leads to SPI/GL bioplastics with higher Young Modulus. This effect coincides with the increase in bending elastic modulus [Figure 3(A)], being moderate in this case. No significant differences have been found for the rest of parameters that show a poor repeatability. In any case, these results agree with the idea that higher pressure leads to a higher degree of orientation. If we observe a SEM photographs for selected samples processed at 500 and 900 bars [Figure 8(A,C)] it is possible to observe how the sample processed at higher pressure show a more homogeneous appearance.

Table III. Water Uptake Capacity for SPI/Gly 50/50 Obtained through Injection Molding at Different Processing Conditions

		Water uptake (%)	Soluble matter loss (%)
Cylinder temperature	40 °C	688 ± 32	54.9 ± 0.1
	80 °C	620 ± 7	56.5 ± 0.3
	120 °C	386 ± 3	54.9 ± 0.2
Injection pressure	300 bar	553 ± 60	50.9 ± 0.3
	500 bar	688 ± 32	54.9 ± 0.1
	900 bar	546 ± 32	52.4 ± 0.3
Mold temperature	60 °C	711 ± 21	55 ± 1
	70 °C	688 ± 32	54.9 ± 0.1
	80 °C	586 ± 25	55 ± 1
	90 °C	564 ± 44	53 ± 1
	130 °C	213 ± 13	49.1 ± 0.1

Figure 7(B) shows the values of E, σ_{max}, and ε_{max} from tensile tests performed on SPI/GL bioplastic specimens, as a function of mold temperature. Generally, higher tensile parameters are obtained (σ_{max}, ε_{max}, and E) when mold temperature becomes higher, although no significant differences can be observed between 70 and 80 °C. A change in behavior takes place for σ_{max} and E that undergo a significant decrease from 90 to 130 °C. On the other hand, a remarkable increase takes place for ε_{max}. Thus the maximum elongational strain at a mold temperature of 130 °C becomes six times higher than its value at 60 °C, although at the expense of a reduction in tensile strength. Pateau *et al.*[32] also obtained higher values for ε_{max} when increasing the molding temperature from 80 to 140 °C for soy isolate bioplastics processed through compression, although they reported an increase in σ_{max} as well. A similar evolution for σ_{max} with increasing molding temperature of soy protein specimens was reported by Mo *et al.*,[16] who also found a maximum in ε_{max}. In any case, the subsequent decrease in both parameters took place at molding temperatures higher (>140 °C) than those used in this study.

The enhancement in tensile parameters may be explained since high molding temperatures allow higher polymer chains mobility, which eventually may enhance the flow properties of the material and improve the alignment and interaction of the chains.[32,33] However, the change in the evolution trend from 90 to 130 °C, suggests a change towards an elastomeric-like behavior characterized by a certain crosslinking degree that essentially favor elongation.

In addition, the above mentioned change in behavior shown at temperatures above 90 °C also coincides with a modification in the visual appearance of SPI/GL specimens. These specimens were powder-like white yellow from 60 to 90 °C and dark brown translucent at 130 °C. Similar evolution of visual appearance patterns was reported by Mo *et al.*[16] and Cunningham *et al.*[34]

Water Uptake

There has been an increase in the number of research studies concerning water uptake capacity in biopolymer systems during the last years, specially due to their potential applications in the fields of biomedical, pharmaceutical, environmental, and agricultural engineering.[34–38]

Table III shows the values of water uptake obtained for SPI/GL specimens after 24 h immersion, determined according to the procedure described in the "Experimental" section, as a function of the three processing parameters considered: cylinder temperature, injection pressure, and mold temperature. In any case, it is noteworthy how all the bioplastic samples show high values of water uptake (above 200%), which is consistent with the results reported by other authors.[16,28] The highly hydrophilic character of soybean protein seems to provide these soy-based materials with a high capacity to absorb water into its structure, which makes these formulations an interesting starting point to potentially develop optimized superabsorbent materials, especially when compared to other vegetable proteins as wheat gluten[23] or pea protein.[39]

An increase in the cylinder temperature results in a decrease in the water uptake capacity, which is only significant when temperature is higher than 80 °C (e.g., 120 °C). At these higher temperatures, water uptake may achieve values approximately half of those obtained originally (as compared to 40 °C). When observing the SEM photographs of samples processed at different cylinder temperature values (Figure 8), microstructure is found to be completely different, showing a more aligned structure for the sample injected at 120 °C [Figure 8(D)] when compared with the sample injected at 40 °C [Figure 8(A)]. It seems that the role of glycerol is also quite dependent on the cylinder temperature. Thus, phase segregation is more apparent at 40 °C, where the glycerol-rich phase is randomly dispersed as filler all over the protein matrix. In contrast, at 120 °C, a much lower degree of segregation takes place, being limited to some narrow rodlike regions. As a result, the typical plasticizing behavior of glycerol seems to dominate, being distributed within the protein matrix. The difference found between the visual appearances for both samples confirm the abovementioned different behavior. At 40 °C the specimens display cream color with a fairly opaque appearance, whereas they acquire amber-like color, becoming slightly transparent, when using 120 °C as the cylinder temperature. This is indicative of a higher amorphous character related to an improved plasticizing efficiency.

Regarding the effect of the injection pressure, the water uptake displays maximum values for the specimens processed at 500 bar. This is also the pressure at which the loss of soluble matter becomes higher. It may be noticed that an increase in pressure from 300 bar (either to 500 or 900 bar) leads to an increase in this parameter, even exceeding the glycerol content (ca. 50%). In other words, the increase in pressure favors the loss of some protein together with glycerol, particularly from 300 to 500 bar. As mentioned in "DMA" section, an increase in pressure also involves an increase in the density of the specimen. As a result of both effects, the amount of protein remaining after immersion in water for 24 h becomes minimum for the specimen processed at 500 bar. Therefore, it may be assumed that this is the specimen having the highest void fraction after 24 h immersion, which explains its highest water absorption capacity. The decrease in water uptake from 500 to 900 bar may be also regarded as a consequence of a greater packing of the protein matrix, which is consistent with the increase in elasticity (E' and Young modulus) and with the evolution observed in SEM and physical appearance images [Figure 8(A,C)]

The mold temperature is the processing variable that exerts the greatest effect on water uptake, keeping both the cylinder temperature and the injection pressure constant at those values where water uptake was higher (40 °C and 500 bars, respectively). As may be observed in Table III, a remarkable increase in the water uptake capacity is obtained by decreasing the mold temperature. This evolution fits a linear relationship ($R^2=0.98$), according to the following equation:

$$W = a - b \cdot T_m$$

where W is the water uptake percentage and T_m is the mold temperature.

A quantitatively similar behavior, although showing slightly lower values, has been found at higher cylinder temperature (results not shown).

These results suggest that an increase in the mold temperature progressively promotes protein crosslinking, leading to an enhancement of the protein network, which eventually may result in a closely packed structure. Pateau *et al.*,[32] reported a similar effect with soy protein/water bioplastics. Zarate-Ramírez *et al.*[23] also observed a similar evolution when studying the effect of mold temperature in gluten bioplastics. However, in both cases water uptake yielded much lower values. Table III also shows how the loss soluble matter is reduced down to the amount of glycerol when the mold temperature is highest. This support the above-mentioned evolution in protein crosslinking driven by the mold temperature, that even reaches the point of completely preventing protein to be extracted through water immersion. These results are also consistent with the increase in bending and tensile elasticity induced by the mold temperature.

CONCLUSIONS

50/50 SPI/glycerol mixtures may be processed through a wide processing conditions window, as may be deduced from temperature ramp dynamic bending tests. Thus, temperatures as low as 40 °C and as high as 130 °C were considered for the cylinder and mold temperature, respectively.

Bending properties of the SPI/glycerol injection molded bioplastics are not as sensitive to changes in the processing conditions studied as tensile properties or water uptake capacity. Thus, all soy-based bioplastics display a thermoplastic behavior, with a glass transition around 50–75 °C that seems to correspond to protein-rich domains.

Furthermore, processing bioplastics at higher temperatures or pressure yields higher values for the Young modulus, which has been related to a higher degree of crosslinking. Increasing mold temperature from 60 to 130 °C also leads to a higher extensibility of bioplastic samples when submitted to a uniaxial tensile load.

All the bioplastic samples show remarkably high values of water uptake, ranging from 200% to 700%. Low cylinder temperatures (e.g., 40 °C), medium injection pressures (e.g., 500 bars) and low mold temperatures (e.g., 60 °C) generally lead to higher water uptake capacities, as higher values would result in a closely packed structure.

Apparently, from these results it seems that a higher structuration in the system favors the elasticity of the material but also reduces considerably its water uptake capacity. Thus, when searching for a material with an optimized water uptake capacity, it may be interesting to use softer processing conditions, especially molding temperatures lower than 90 °C. In this sense, it may be concluded that SPI-based bioplastics may be regarded as promising materials for absorbent applications.

ACKNOWLEDGMENTS

The authors acknowledge the financial support from the MICINN/FEDER (MAT2011-29275-C02-02). The authors also gratefully acknowledge to CITIUS (University of Sevilla) for providing full access and assistance to the Microscopy Service.

REFERENCES

1. Chen, P.; Zhang, L. *Macromol. Biosci.* **2005**, *5*, 237.
2. Brooks, J. R.; Morr, C. V. *J. Am. Oil Chem. Soc.* **1985**, *62*, 1347.
3. Zhang, J.; Mungara, P.; Jane, J. *J. Polym.* **2001**, *42*, 2569.
4. Reddy, M. M.; Misra, M.; Mohanty, A. K. *J. Mater. Sci.* **2011**, *47*, 2591.
5. Garcia, M. C.; Torre, M.; Marina, M. L.; Laborda, F. *Rev. Food Sci. Nutr.* **1997**, *37*, 361.
6. Kumar, R.; Choudhary, V.; Mishra, S.; Varma, I. K.; Mattiason, B. *Ind. Crop Prod.* **2002**, *16*, 155.
7. Pommet, M.; Redl, A.; Morel, M. H.; Guilbert, S. *Polymer* **2003**, *44*, 115.
8. Song, F.; Tang, D.; Wang, X.; Wang, Y. *Biomacromolecules* **2011**, *12*, 3369.
9. Irissin-Mangat, J.; Gerard, R.; Bernard, B.; Gontard, N. *Eur. Polym. J.* **2001**, *37*, 1533.

10. Matveev, Y.; Guinberg, V.; Tolstoguzov, V. *Food Hydrocolloid* **2000**, *14*, 425.
11. Pouplin, M.; Redl, A.; Gontard, N. *J. Agric. Food Chem.* **1999**, *47*, 538.
12. Lieberman, E. R.; Gilbert, S. G. *J. Polym. Sci. Polym. Symp.* **1973**, *41*, 33.
13. Guerrero, P.; Retegi, A.; Gabilondo, N.; De la Caba, K. *J. Food Eng.* **2010**, *100*, 145.
14. Félix, M.; Martínez-Alfonso, J. E.; Romero, A.; Guerrero, A. *J. Food Eng.* **2014**, *125*, 7.
15. Adamy, M.; Verbeek, C. J. R. *Adv. Polym. Technol.* **2013**, *32*, 1.
16. Mo, X.; Sun, X. S.; Wang, Y. *J. Appl. Polym. Sci.* **1999**, *73*, 2595.
17. Huang, M. C.; Tai, C. C. *J. Mater. Process. Technol.* **2001**, *110*, 1.
18. Mohanty, A. K.; Tummala, P.; Liu, W.; Misra, M.; Mulukutla, P. V.; Drzal, L. T. *J. Polym. Environ.* **2005**, *13*, 279.
19. Tummala, P.; Liu, W.; Drzal, L. T.; Mohanty, A. K.; Misra, M. *Ind. Eng. Chem. Res.* **2006**, *45*, 7491.
20. Liu, W.; Misra, M.; Askeland, P.; Drzal, L. T.; Mohanty, A. K. *Polymer* **2005**, *46*, 2710.
21. Van Wazer, J. R.; Lyons, J. W.; Kim, K. Y.; Colwell, R. E. In: A Laboratory Handbook of Rheology; Schierbauni, F. Ed., Interscience Publishers: New York, **1963**; p 187.
22. Dealy, J. M. Rheometers for Molten Plastics: A Practical Guide to Testing and Property Measurement; Van Nostrand Reinhold Co.: New York, **1982**, p 255.
23. Zarate-Ramírez, L. S.; Martínez, I.; Romero, A.; Partal, P.; Guerrero, A. *J. Sci. Food Agric.* **2011**, *91*, 625.
24. Fernández-Espada, L.; Bengoechea, C.; Cordobés, F.; Guerrero, A. *Food Bioprod. Process.* **2013**, *91*, 319.
25. Orawan, J.; Soottawat, B.; Wonnup, V. *Food Hydrocolloid* **2006**, *20*, 1153.
26. Jerez, A.; Partal, P.; Martinez, I.; Gallegos, C.; Guerrero, A. *Rheol. Acta* **2007**, *46*, 711.
27. Ogale, A. A.; Cunningham, P.; Dawson, P. L.; Acton, J. C. *J. Food Sci.* **2000**, *65*, 672.
28. Chen, P.; Zhang, L.; Cao, F. *Macromol. Biosci.* **2005**, *5*, 872.
29. Tian, H.; Wu, W.; Guo, G.; Gaolun, B.; Jia, Q.; Xiang, A. *J. Food Eng.* **2012**, *109*, 496.
30. Kalichevsky, M. T.; Jaroszkiewicz, E. M.; Blanshard, J. M. V. *Int. J. Biol. Macromol.* **1992**, *14*, 257.
31. Pateau, I.; Chen, C. Z.; Jane, J. *Ind. Eng. Chem.* **1994**, *33*, 1821.
32. McCrum, N. G.; Buckley, C. P.; Bucknell, C. B. Principles of Polymer Engineering, 2nd ed.; Oxford University Press: New York, **1997**, p 7.
33. Cunningham, P.; Ogale, A. A.; Dawson, P. L.; Acton, J. C. *J. Food Sci.* **2000**, *65*, 668.
34. Buchholz, F. L.; Graham, A. T. Modern Superabsorbent Polymer Technology; Wiley-VCH: New York, **1998**.
35. Castro, G. R.; Panilaitis, B.; Kaplan, D. L. *Bioresour. Technol.* **2008**, *99*, 4566.
36. Gómez-Martínez, D.; Partal, P.; Martínez, I.; Gallegos, C. *Ind. Crops Prod.* **2013**, *43*, 704.
37. Yang, L.; Yang, Y.; Chen, Z.; Guo, C.; Li, S. Ecol. Eng. **2014**, *62*, 27–32.
38. Li, X.; He, J.; Hughes, J.; Liu, Y.; Zheng, Y. *Appl. Soil Ecol.* **2014**, *73*, 58.
39. Tömösközi, S.; Lásztity, R.; Haraszi, R.; Baticz, O. *Nahrung Food* **2001**, *45*, 399.